applied sciences

MDPI

Article

Energy Harvester Based on a Rotational Pendulum Supported with FEM

Grzegorz Litak [1,*], Mirosław Kondratiuk [2], Piotr Wolszczak [1], Bartłomiej Ambrożkiewicz [1] and Abhijeet M. Giri [1]

[1] Faculty of Mechanical Engineering, Lublin University of Technology, Nadbystrzycka 36, 20-618 Lublin, Poland; p.wolszczak@pollub.pl (P.W.); b.ambrozkiewicz@pollub.pl (B.A.); a.giri@pollub.pl (A.M.G.)

[2] Faculty of Mechanical Engineering, Białystok University of Technology, Wiejska 45C, 15-351 Białystok, Poland; m.kondratiuk@pb.edu.pl

* Correspondence: g.litak@pollub.pl

Abstract: The proposed energy harvesting system is based on a rotational pendulum-like electromagnetic device. Pendulum energy harvesting systems can be used to generate power for wearable devices such as smart watches and fitness trackers, by harnessing the energy from the human body motion. These systems can also be used to power low-energy-consuming sensors and monitoring devices in industrial settings where consistent ambient vibrations are present, enabling continuous operation without any need for frequent battery replacements. The pendulum-based energy harvester presented in this work was equipped with additional adjustable permanent magnets placed inside the induction coils, governing the movement of the pendulum. This research pioneers a novel electromagnetic energy harvester design that offers customizable potential configurations. Such a design was realized using the 3D printing method for enhanced precision, and analyzed using the finite element method (FEM). The reduced dynamic model was derived for a real-size device and FEM-based simulations were carried out to estimate the distribution and interaction of the magnetic field. Dynamic simulations were performed for the selected magnet configurations of the system. Power output analyses are presented for systems with and without the additional magnets inside the coils. The primary outcome of this research demonstrates the importance of optimization of geometric configuration. Such an optimization was exercised here by strategically choosing the size and positioning of the magnets, which significantly enhanced energy harvesting performance by facilitating easier passage of the pendulum through magnetic barriers.

Keywords: vibration energy harvesting; FEM in electromagnetism; pendulum system

check for updates

Citation: Litak, G.; Kondratiuk, M.; Wolszczak, P.; Ambrożkiewicz, B.; Giri, A.M. Energy Harvester Based on a Rotational Pendulum Supported with FEM. *Appl. Sci.* **2024**, *14*, 3265. https://doi.org/10.3390/app14083265

Academic Editor: Andreas Sumper

Received: 5 March 2024
Revised: 3 April 2024
Accepted: 11 April 2024
Published: 12 April 2024

1. Introduction

Small- and micro-scale energy harvesting (EH) usually refers to the conversion of ambient energy from different sources, including mechanical vibration energy, into electrical energy, which can be further accumulated or used for powering up devices demanding low amounts of energy [1,2]. One of the main advantages of such energy harvesting systems is the capability of onsite energy transduction and power supply for the integrated operation of small- and microelectronic devices. EH systems can also be used for remote and inaccessible locations or maintenance-free applications [3,4]. Another advantage is the improvement in the efficiency of the parent process, which acts as an ambient energy source, due to recovery of energy which could be otherwise lost [x1]. These energy harvesting systems can readily contribute to the current industrial revolution called Industry 4.0 or the internet of things (IoT) [5,6], which demand independent sources of energy for powering up electronic units and sensors. In general, such EH systems are classified as per the source of ambient energy, i.e., mechanical vibrations, thermal, solar, wind, radio waves (RF), fluid motion, etc. (see Figure 1). Many devices have been developed by researchers based on the abovementioned energy sources. In this research work, we focused on energy conversion from ambient mechanical vibrations using a pendulum-like rotating body with modifications possible in the system's potential [7].

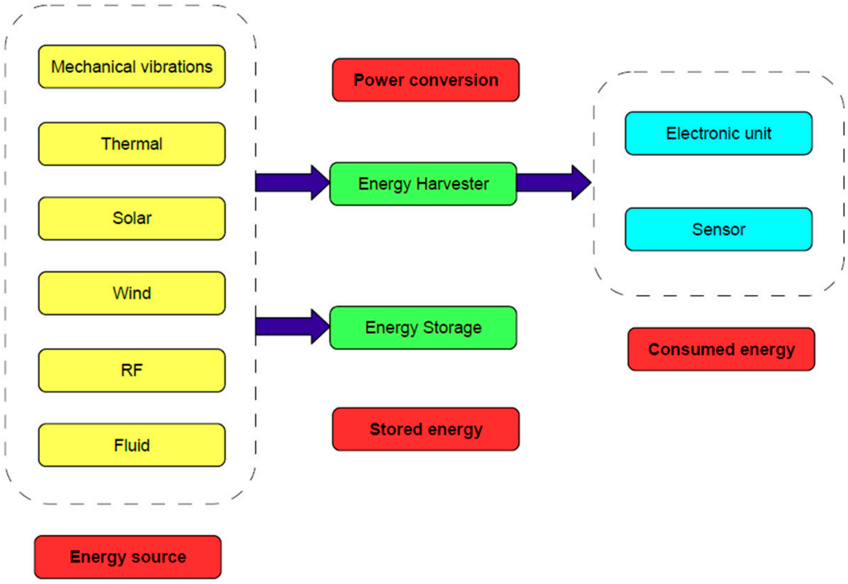

Figure 1. The energy conversion process in the energy harvesting systems.

It is worth mentioning that energy harvesting systems that are based on ambient mechanical vibrations are generally divided into electromagnetic [8,9], piezoelectric [10,11], and electrostatic [12,13] categories. In many scientific articles, they are called vibration energy harvesters (VEH) [14,15]. VEH systems have gained popularity because they provide the simplest transduction mechanism and highest efficiency of energy transduction [16,17]. Practical applications of VEH systems span diverse sectors. In the automotive industry, these systems can capture energy from vehicle vibrations to power tire pressure monitoring systems or onboard sensors [18]. Similarly, in structural health monitoring, they can be employed to generate power for sensors embedded in bridges or buildings while facilitating continuous monitoring. This eliminates the need for frequent battery replacements as well [19]. Furthermore, wearable devices [20] can utilize VEH system to extend battery life or even eliminate the need for batteries altogether, enhancing user convenience and sustainability.

Being a linear dynamic system, a simple VEH responds well only when excited near its resonance frequency. This is a major disadvantage because the harvested power from the device drops when excited at other non-resonant operational frequencies resulting from uncertain ambient conditions [21]. However, to overcome this problem, many current research works are focusing on the broadband frequency-response effect to build a flexible system adjusting to the wider range of operational frequencies [22–24]. Compared to a linear system, the broadband frequency effect causes a reduction in the mechanical quality factor (Q-factor). The highest power output obtained under resonant conditions also reduces because a nonlinear system may exhibit multiple low- and high-amplitude solutions [25–27]. However, as the nonlinear systems exhibit better performance at non-resonant conditions, overall harvesting efficiency is improved due to the broadband response. Such nonlinear behavior has been obtained by using nonlinear mechanical and magnetic springs with softening or hardening effects [28]. Some of the interesting proposals include energy harvesters with multi-stable mechanical or magnetic potential [29–32]. A few other approaches involve active and autonomous tuning of system parameters to sustain the resonance conditions [33,34].

Until now, many VEH systems have been explored based on their applications, source of excitation, and transduction methods, with the primary objective of improving efficiency and broadband response. One of the recent trends is to improve performance by introducing different types of nonlinearities into the system. Concurrently, studies to support experiments with mathematical modeling and numerical simulations are also being undertaken. Numerical simulations using finite element analysis (FEA) show potential for nonlinear modeling and are capable of revealing the future directions in this field.

2. The Concept of Pendulum-Based Electromagnetic Energy Harvesting Systems

In recent times, energy harvesting systems using rotational movement have been receiving attention to scavenge energy from the environment [34–37]. Very often, pendulums are used in electromagnetic energy harvesting systems because they allow versatility in their configuration. Electromagnetic transduction of vibration energy in the standard magnet–coil generators is based on the electromagnetic induction phenomena. In this, electromotive force is induced in an induction coil, which cuts the magnetic flux of a core during its relative displacement. For improving the electromagnetic coupling with the strongest flux density, permanent magnets made from an alloy of neodymium, iron, and boron (NdFeB) are most suitable. These magnets are also available in various configurations based on the direction of polarization, shapes, sizes, grades of neodymium, and thermal resistance.

Historically, many concepts of electromagnetic energy harvesting systems with pendulums have been proposed among the other types of low-frequency energy harvesting systems based on cantilevers, mechanical springs, magnetic springs, and spiral springs [38]. Electromagnetic pendulum-based harvesters can depict both oscillations and full rotation of the pendulum depending on the character of excitation. In real applications, a particular design faces challenges such as sustaining rotational motion under random excitations, and sizing of the system based on constraints or power supply requirements [39]. In order to overcome such challenges and optimize the system for a particular application, several modifications were introduced. These modifications were based on the research on mechanical couplings [40,41], using sub-harmonic resonance for the broadband power output [42], and using nonlinearities as an additional source of energy [43].

One of the analysis approaches used to study the dynamics of EH systems is comparing the experimental results with the results of mathematical modeling. Simplified mechanical models based on spring-mass systems have provided fairly good results in many studies [44–46]. Another approach is using the FEA for analyzing the electromagnetic interactions in such systems [47–49]. Currently, several commercial FEA software packages are available for analyzing electromagnetism problems including 2D axis-symmetric problems and advanced 3D problems. Some of the popular FEA programs are NEC (Numerical Electromagnetics Code), FEKO (Altair Engineering), COMSOL Multiphysics (COMSOL Inc.), and Momentum (Keysight EEsof EDA).

Referring to the study on electromagnetic energy harvesters using rotational movement [7], we propose a rotational pendulum concept with an improved approximation. The originality of this system is the variable potential introduced by the pairs of additional adjustable magnets whose strength can be changed. The dynamic response of this system, depending on the system's configuration, provides full rotation or oscillations of the pendulum, which in turn influences the output power. In our analysis, we studied the magnetic interactions and the dynamics of a system using the FEA and mathematical models. In our previous work [7], the effect on performance was analyzed through magnetic interactions with a simplified FEA model. In this study, the effect of magnet positioning on potential modulation and on attaining complete rotational response is explored using numerical simulations. To avoid magnetic interaction with the housing, the system was realized using the 3D printing technique. The originality of the concept lies in the incorporation of adjustable additional magnets to modulate the magnetic potential, allowing a customizable system configuration that improves both pendulum dynamics and output power.

This article is organized in the following way. In the next section (Section 3), the proposed concept of the rotational VEH system with the pendulum is described. Mathematical models of the electromagnetic EH system, with inputs from the FEA, are introduced and described. Further, details about the experiment and measuring circuit are given. In Section 4, dynamics of the pendulum caused by different configurations of additional magnets are discussed and visualized with the results of numerical simulations. Lastly, Section 5 summarizes and provides conclusions of this analysis.

3. Design and Modeling of an Energy Harvesting System with a Rotational Pendulum

In electromagnetic energy harvesting systems, the voltage is induced in coils according to Faraday's law by the changing of the magnetic flux in the coils. In this pendulum-based electromagnetic EH system, modulation of magnetic potential using the alignment of additional magnets is proposed. In the analyzed prototype, the adjustable potential is produced by two symmetrically mounted magnetic pairs (see Figure 2), changing the character of the system. This EH system was designed entirely with non-magnetic or weak magnetic materials using 3D printing (ABS—acrylonitrile butadiene styrene), plastic (nylon), and aluminum; the motivation was to avoid undesirable magnetic interaction with the system's other parts. Optionally, external pendulums can also be attached to the system on its sides to increase the moment of inertia and to overcome potential barriers by full rotations. The magnetic-electrical circuit consisted of 12 magnetic coils connected in series and two types of permanent magnets, one in the form of the tip mass mounted at the end of the pendulum and two pairs of adjustable magnets placed inside the plastic housing tunnels (Figure 3).

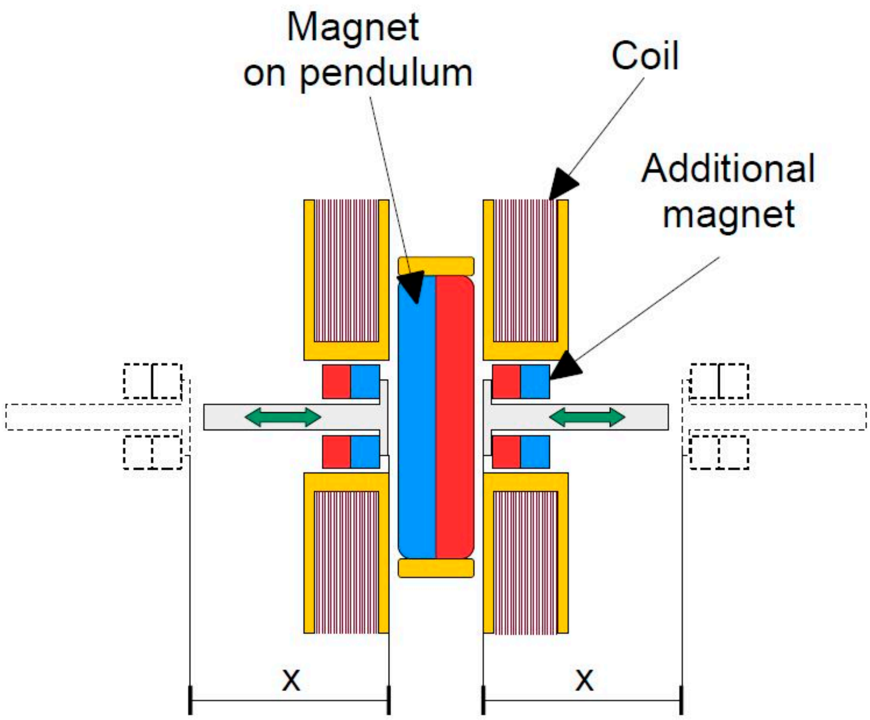

Figure 2. Magnetic interaction in the energy harvester. The additional magnets are movable axially, which changes the magnetic force between permanent magnets. The maximum distance by which the additional magnet can be moved axially is x = 13 mm.

A compact EH system was designed here by limiting the system's dimensions to 10 cm in any direction from the center (see Figure 3a). The design allowed for versatile coil connections; for example, we connected six coils on a single wall of the system. Within these coils, we strategically placed four additional adjustable permanent magnets—two on each side of the system (Figure 3b). These magnets played a crucial role in electromagnetic induction within the system and influenced the movement of the pendulum by creating a double potential well.

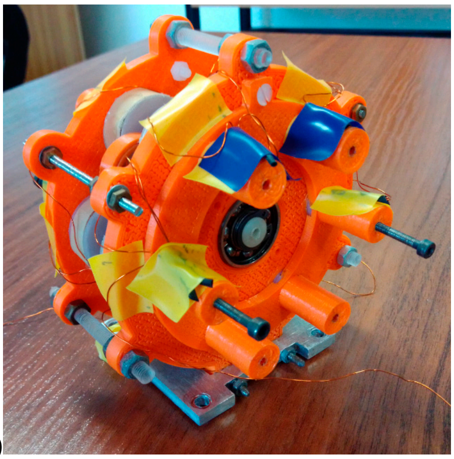
(a)
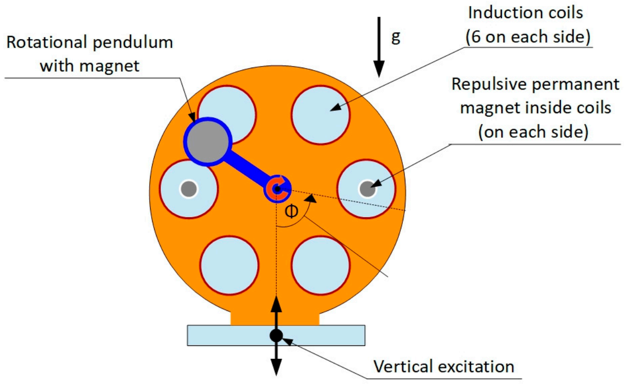

(b)

Figure 3. The physical concept of the electromagnetic energy harvesting system with rotational pendulum: (**a**) physical prototype view; (**b**) the scheme of the system (cross-section view).

Mechanical and electrical properties of this EH system are listed in Table 1. More information on the technical issues of such EH systems can be found in [49], in which experiments and the simplified FEA (2D planar) are described. As this study will combine two-stage modeling, i.e., a 3D FEM electromagnetic model and simulating the mathematical model using MATLAB (v2022b) software, the actual physical quantities of the system are specified in Table 1. Mechanical and electrical features were used for preparation of the 3D model in COMSOL (v5.3) Multiphysics software.

Table 1. Mechanical and electrical properties of the electromagnetic EH system.

Mechanical Part	
Mass of the system (g)	~900
Pendulum magnet (mm)	⌀ 20 (O.D) × 5 (thick) (cylinder)
Side magnets (mm)	⌀ 8 (O.D) × ⌀ 6 (I.D) × 3.5 (thick) (ring)
Diameter of rotation (mm)	⌀ 66.5
Limiting dimensions of the system (mm)	>100
Electrical Part	
Number of coils	12 (connected in series)
Coil induction (mH)	4.545
Number of turns	253
Coil length (mm)	8
Wire type	28 AWG
Resistance (Ω)	30.3
Type of magnets	NdFeB 37

3.1. Electromagnetic FEM Model

In comparison to the previous FEA work in [7], the current system was analyzed in 3D space keeping the existing coil layout and the geometry of the energy harvester (Figure 4). The motivation behind achieving precise calculation using 3D FEA was to obtain the information about the magnetic force between magnets during rotation of the pendulum and its influence on the dynamics of the pendulum with magnet. Once this was obtained, the magnetic torque vector was utilized in the mathematical model. Such magnetic interactions strongly affected the dynamics and changed the energetic potential of the energy harvester [49]. In the finite element (FE) model, the influence of housing can be neglected as the entire housing is made of non-magnetic materials and there are no undesirable external magnetic interactions.

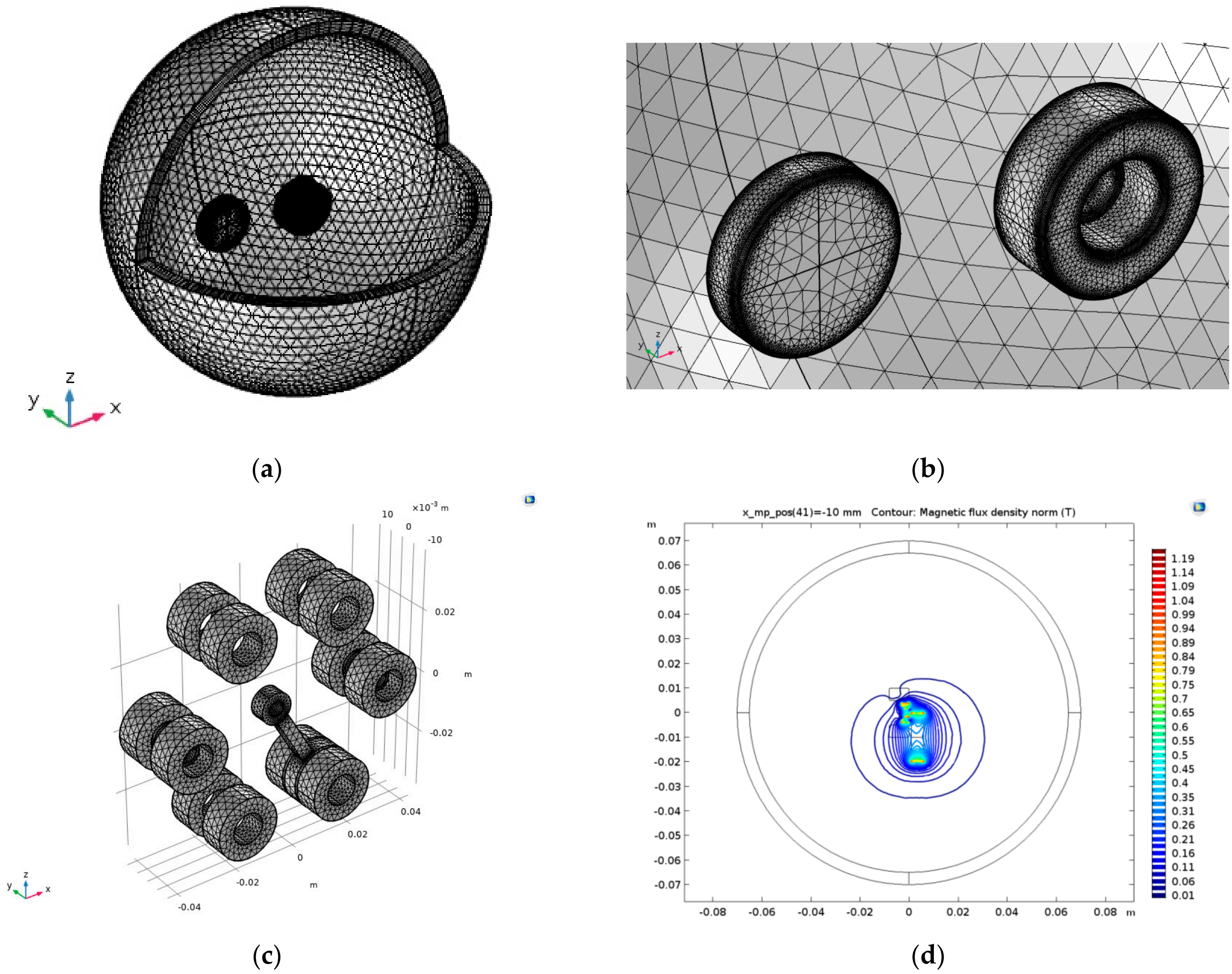

Figure 4. The physical concept of the electromagnetic energy harvesting system with rotational pendulum modeled in COMSOL Multiphysics. (**a**) The entire domain considered for the analysis of magnetic force interaction between pendulum magnet and fixed additional magnet in meshed state. (**b**) Enlarged meshed view of the two interacting magnets mentioned above. (**c**) Meshed geometry considered for the MBD analysis of the system, and (**d**) the distribution of the magnetic field during interactions between the magnets shown in the top planer view of (**b**) (directly taken from the COMSOL results report).

The current problem is a typical multi-body dynamics (MBD) problem dealing with the combination of the dynamics and electromagnetism. Additionally, an electrical circuit was added to analyze the power output of the system. Moreover, couplings between the magnet–magnet and magnet–coil pairs were investigated in the form of acting forces and torques. Thus, the obtained torque vector using FEA was crucial for the analysis of the pendulum's dynamics. As the FEA model was linear, the system could be analyzed for one rotation of the pendulum. Hence, the results were obtained for one rotation per second of the pendulum.

In order to obtain magnetic force interaction between the pendulum magnet and the additional fixed magnet using FEA, a stationary model was considered, as shown by a meshed view in Figure 4a. In this view, the relative size and positions of the magnets as well as the surrounding air space considered for the magnetic interaction is shown. The linear position of the pendulum magnet relative to the additional magnet–coil pair was changed along the x-axis (see Figure 4b), from which the magnet force in terms of x-, y-, and z-axis components was computed. A detailed description of this procedure is mentioned in the attached Supplementary Materials to this article. Further, using these calculations, resultant magnet forces and torques for magnet–magnet and magnet–coil pairs were estimated. These force and torque quantities along with the electrical variables were then considered for the MBD analyses of the system shown Figure 4c. A top view of Figure 4b showing magnetic flux interaction between the magnets is shown in Figure 4d. Readers can find the geometric dimensions and other physical variables used for these FEM simulations in the Supplementary Materials attached with this article.

3.2. Reduced Mathematical Model

In Figure 5, the scheme of the mathematical model for the energy harvester with terms applied in the equation of motion is presented. Vertical excitation coming from the shaker initiated the movement of the rotational pendulum around the pivot in the form of oscillations or full rotations, depending on the applied strength of excitation and the strength of magnetic interactions in the system. The mentioned terms had significant influence on the system's response, which is discussed in the next section. In Table 2, the values of the terms used in the mathematical model are listed.

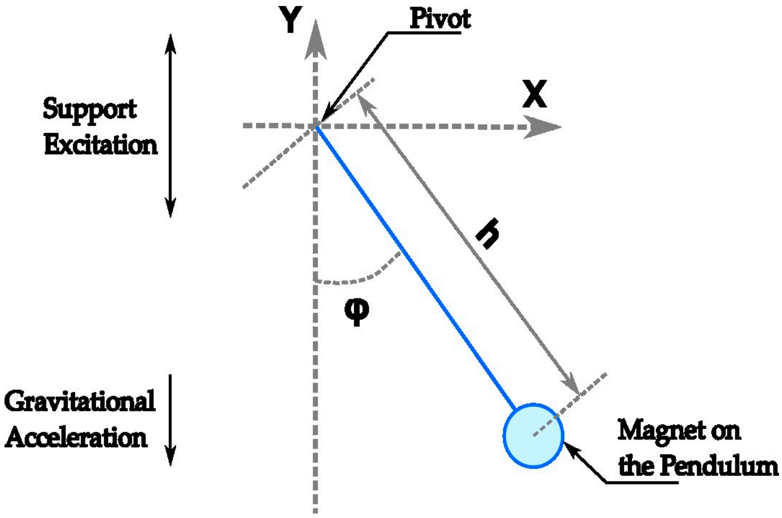

Figure 5. Variables in the mathematical model are shown in the simplified configuration of the energy harvester with magnetic pendulum.

Table 2. Parameters used in the mathematical model (see Equation (1)).

Term	Value
I [kg-m^2]	0.000377
m [kg]	0.0186
g [m/s^2]	9.81
h [m]	0.03325
α, β	0 and 1
λ	0.048
h [m]	0.034
ω [rad/s]	15
A [m]	0.2

In comparison with the previously derived mathematical model of the rotational pendulum [7], additional terms were added, which consider magnet–magnet and magnet–coil couplings. Relative displacement between the pendulum magnet and permanent magnet pair in its proximity created strong magnetic interactions in the form of two opposite potential wells, affecting the acting magnetic forces in the system, as can be observed in Figure 6a. During the relative displacement between magnets, the peak-to-peak amplitude of the pendulum's torque changed drastically, creating a direct influence on its dynamics. The coupling between the pendulum's magnet and the coils had a periodic response (Figure 6b) in each of the 12 coils, showing a relatively smaller impact on its dynamics. Thus, the governing equation of motion (Equation (1)) for the pendulum considering these additional forces can be expressed in the following form:

$$\ddot{\varphi} + \frac{1}{I}\left(c\dot{\varphi} - \alpha F_{mc}(\varphi)\dot{\varphi} + mgh\sin(\varphi) - \beta F_{mm}(\varphi) - m\omega^2 Ah\,sin(\varphi)\cos(\omega t)\right) = 0, \quad (1)$$

where I—moment of inertia of the pendulum, m—mass of pendulum and additional inertial masses, g—gravitational acceleration, h—distance from center of gravity to pivot axis, F_{mc}—torque between magnet–coil couplings obtained with FEA, ω—angular velocity of the pendulum, A—amplitude of the vertical excitation, F_{mm}—torque between magnet–magnet couplings in the system obtained with FEA, c—coefficient of mechanical damping (in the calculations we assumed $c = 0$ for simplicity), α, β = 0 or 1—are the coefficients of magnetic force that are dependent on the distances between magnets and coils. We have neglected the macroscopic eddy currents in the magnets.

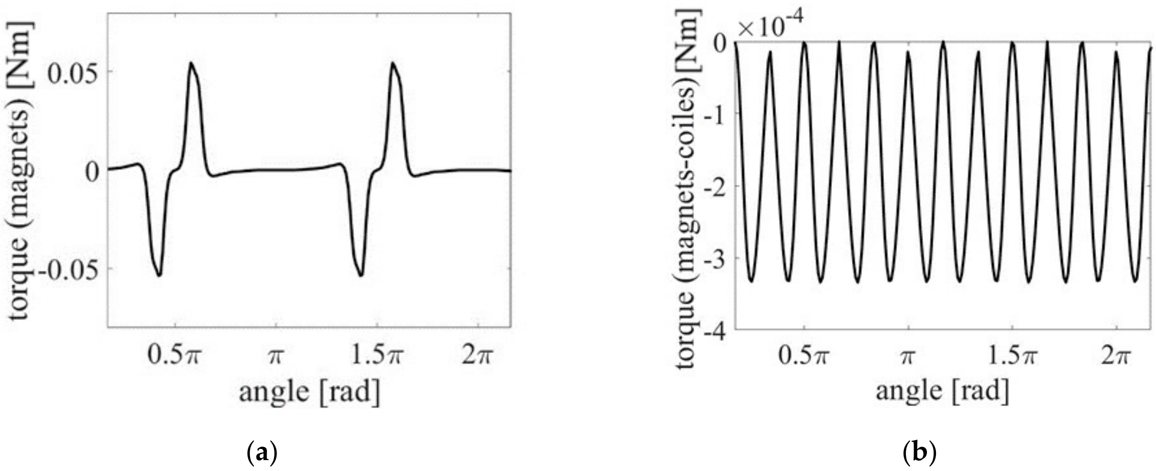

Figure 6. (**a**) The torque from magnet–magnet coupling F_{mm} [Nm] (see Equation (1)) calculated with the FEM model. (**b**) The torque from magnet–coil F_{mc} coupling [Nm] (see Equation (1)) during the clockwise rotation of the pendulum with a constant rotational velocity (1 revolution per second). The initial angle in FEM calculations was 0.25π.

The output power of the system in time domain t is calculated using the following formula (Equation (2)):

$$P = \frac{1}{R_l}\frac{1}{t}\int_0^t U^2(t)dt = (1-\lambda)\alpha F_{mc}(\varphi)\dot{\varphi}^2, \quad (2)$$

where U is the voltage output estimated on the resistor and $\lambda = R_c/(R_l + R_c)$ is the coil resistivity part of the electrical circuit (R_c and R_l denote coil and load resistances, respectively).

4. Numerical Simulations

The analysis of the influence of magnetic forces on the dynamics of the rotational pendulum started with the FEM computations conducted in the COMSOL (v5.3) Software. In the system, there were two unstable equilibrium points where the axes of moving and additional magnets coincided. The amplitude and the distribution of the magnetic force with the angular position of the rotating pendulum depended on the geometry of the magnets and the distance of their alignment, which were considered in this research. It was observed in the prior work [7] during experiments that the system's frame needed excitation in the specific range of frequencies, i.e., f = 10–15 Hz, in order to obtain a completely rotational solution of the pendulum to attain the highest voltage/power performance. Outside the mentioned range of frequencies, the pendulum became stuck at the equilibrium point and did not move. Additionally, it was observed that changing the distance between additional magnets mounted on the sides influenced the potential barrier at the equilibrium positions. In this work, the proposed model considers the influence of varying magnetic forces with the alignment distance on the magnetic pendulum. We also focused on solutions with complete rotation of the pendulum.

In the equation of motion, the magnet–magnet and magnet–coil interactions are important terms influencing significantly the dynamics of the pendulum. To estimate these interactions, the 3D model of the energy harvester was meshed for the FEA (Figure 4) and a series of torques was obtained, which are depicted in Figure 6. The FEA results showed the influence of the magnet–magnet interaction was significantly stronger than that of the coil–magnet coupling on the dynamics of the pendulum. Regarding the interactions between the magnet–magnet in the system (Figure 6a), mutually opposite areas with the strongest magnetic interactions were found. Such a repulsive configuration of magnets helps the pendulum to escape from this area if the potential energy is enough to go through the potential barrier created by the magnetic coupling. This is shown by the red dotted lines in Figure 7. For comparison, gravitational potential is also shown by black dotted lines in Figure 7. It had an almost 10 times weaker influence on the pendulum. The magnet–coil couplings (Figure 6b) had smaller amplitude than the magnet–magnet couplings; however, their influence on the pendulum was also considered in this study.

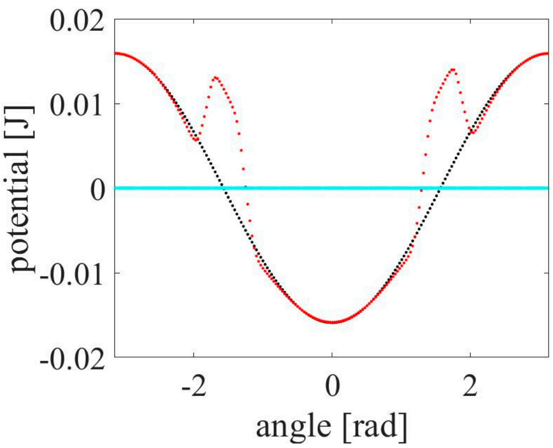

Figure 7. The potential energy of the magnetic force interaction was obtained for one revolution of the pendulum and is shown by the red-dotted line. The potential of the gravity force is shown by a black-dotted line.

We considered the following distinct configurations of the harvester for revealing additional details about the dynamics:

(a) System without coils and without magnets, only pendulum with magnet (only gravitational acceleration): $\alpha = 0$, $\beta = 0$.
(b) System with coils and pendulum with magnet (only magnet–coil coupling): $\alpha = 0$, $\beta = 1$,
(c) System with all magnets and coils.

In Figure 8, the dynamic response of the system is illustrated with the change of angular position Φ and angular velocity ω for the abovementioned different configurations. In all considered cases, the transient state can be observed in the beginning of the system's operation. The reason for this is that the pendulum must first synchronize with the external excitation, and then the steady state operation is observed. For energy harvesting studies, the steady state response is considered from which the highest output voltage/power is observed. In the first case, the system without additional magnets and without coils tended to maintain constant rotations after the synchronization of the pendulum and the vertical excitation. The variations in the angular velocity between positive and negative values depict the pendulum's oscillations around the equilibrium point. Further, the pendulum was able to pass this equilibrium point after around 50 s. Adding induction coils (Figure 8b) established the coil–magnet coupling. The pendulum at first started oscillating, but later when its energy was dissipated by coils, the angular velocity was reduced to zero. Mounting additional magnets strongly influenced the dynamics of the pendulum, which can be seen in Figure 8c. The magnetic force was adjusted by adjusting the axial distance between one of the pair of magnets. Initially, the magnetic potential barrier could not be passed by the pendulum to perform a full rotation. However, after increasing the magnetic force, the repulsive force assisted in easier passing of the magnetic barrier and the pendulum oscillated between the two positions.

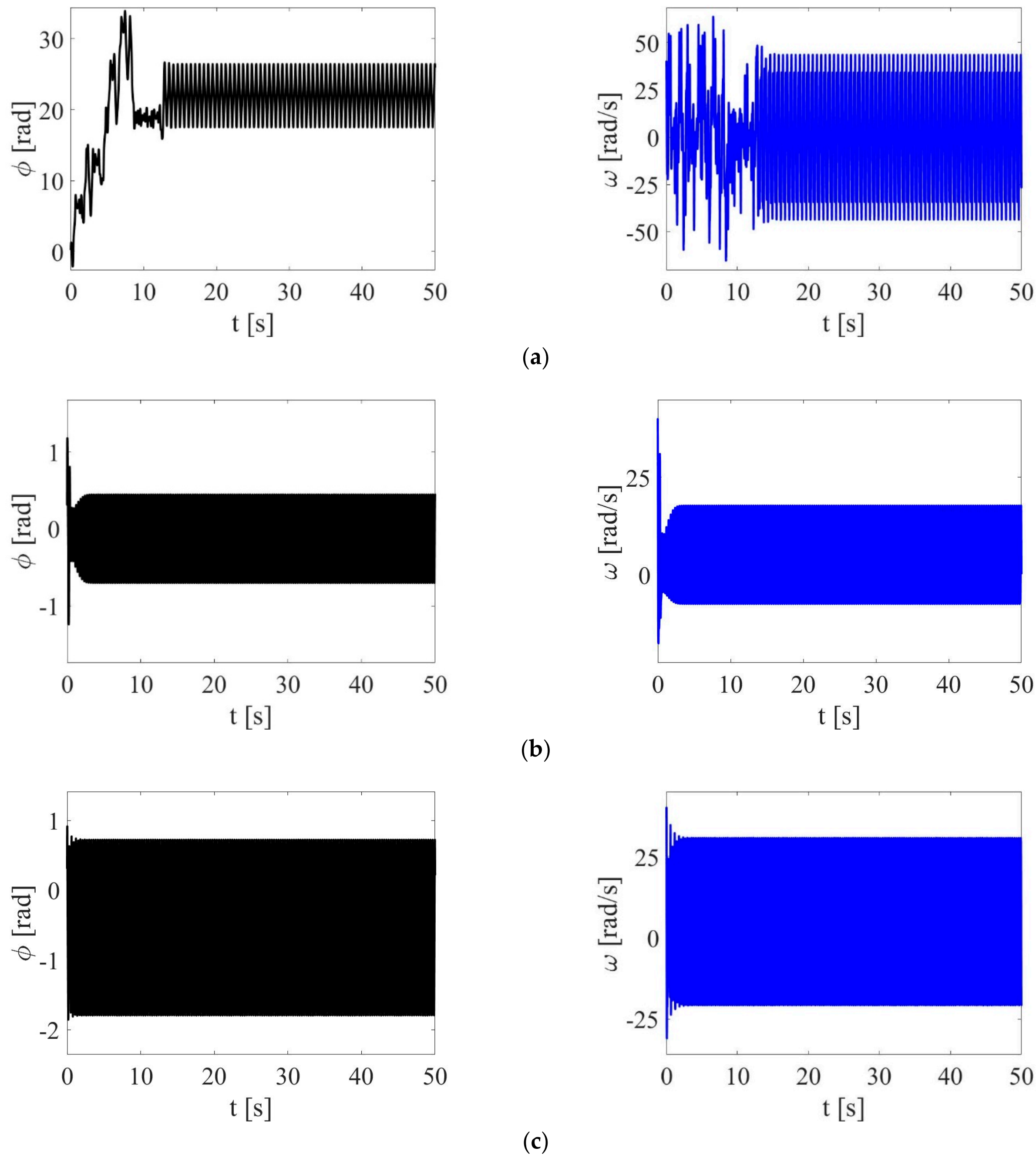

Figure 8. Selected solutions of the dynamic system in terms of the instantaneous rotation angle (left panel—black plots) and angular velocity (right panel—blue plots) of pendulum are shown here. Solutions for (**a**) a system without magnets and coils, (**b**) a system with coils but without additional magnets, and (**c**) a system with additional magnets and coils are presented.

In cases b–c, the voltage in the coils was induced due to the electromagnetic transduction during the parallel passing of the magnet-pendulum around the vicinity of the coils. In Figure 9, the power generated by the pendulum's movement is illustrated. The level of generated power increased as the magnetic force interaction became stronger. The mean value of power was estimated by the moving mean algorithm (see Figure 9—black line), whose value was in the range 0.01–0.02 [W] for case (b). For case (c), the mean harvester power was around 0.5 [W] because of larger and magnetic force-assisted oscillations.

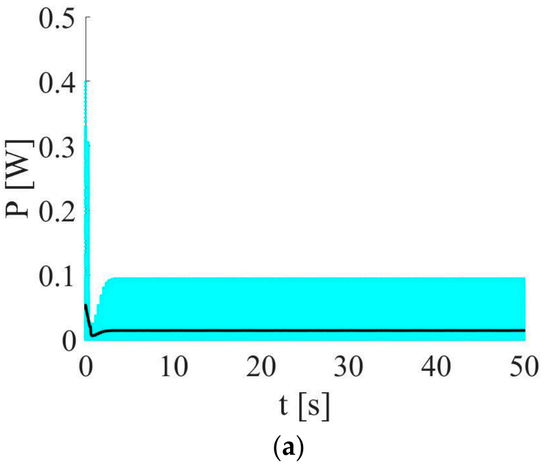

Figure 9. Power output plots corresponding to the solutions of cases (**a**,**b**) (shown in Figure 8b,c, respectively) are shown here. Note, there is no power output in the case shown in Figure 8a, because no electromagnetic transduction occurred in the absence of coils.

The phase portraits of the considered three cases are shown in Figure 10, which illustrates the trajectories drawn by the excited pendulum. Excitation of pendulum without any source of damping caused free rotation under the influence of gravitational potential only (see Figure 10a). After adding coils into the system, its damping caused small amplitude oscillations around the central equilibrium point, as shown in Figure 10b. This was caused by the transduction of energy between the pendulum magnet and coils. Installation of additional magnets led to inter-well oscillations around the offset equilibrium point, where magnetic interactions had maximum impact (see Figure 10c). The phase portrait took a square-based shape and depicted the smaller potential well formed at the specific angular position. It was observed that, as the strength of magnets increased, it became easier to pass through the magnetic barrier at the offset pendulum. Figure 10c shows oscillation of the pendulum between the central and offset equilibrium positions.

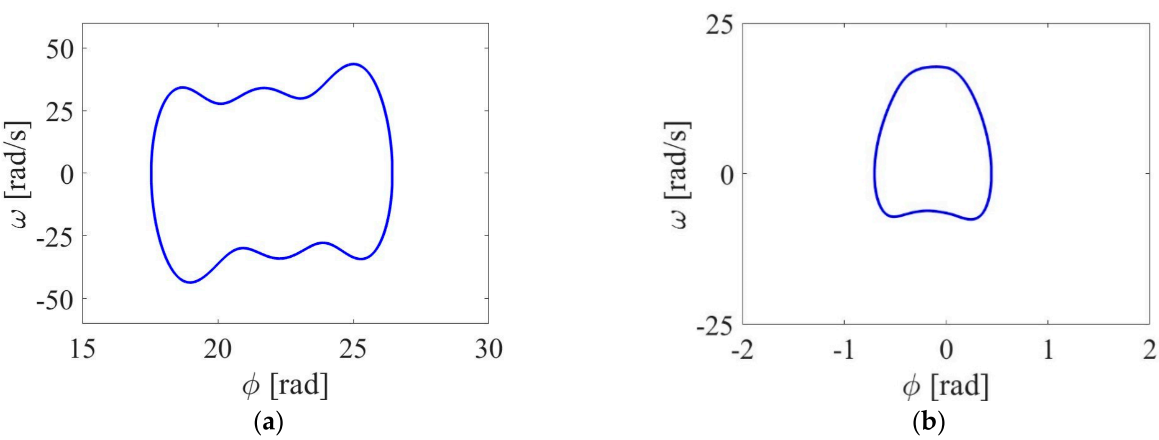

Figure 10. *Cont.*

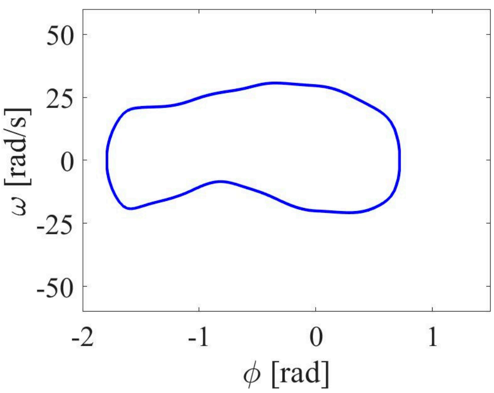

(**c**)

Figure 10. Phase portraits of the considered cases (**a**–**c**) for the solutions shown in Figure 8a–c.

5. Conclusions

This paper investigates the dynamic response of an electromagnetic energy harvester with a rotational pendulum with variable magnetic-force interactions. Based on the concept proposed in [7] with a simplified model, in this work a more rigorous two-stage mathematical model is proposed that includes FEM analysis of magnet–magnet and magnet–coil couplings. The governing equation of motion is presented, which includes the magnetic interaction terms from FEA from the first stage. Based on a physically realized model built using the 3D printing method, physical quantities and terms in the mathematical model were obtained. In this investigation, three majorly different cases were tested, which were configurations with and without coils and magnet couplings, and with adjustable magnet positions. The findings from the constant amplitude excitation experiments highlighted the significant impact of magnetic force on the pendulum's traversal through the magnetic barriers. When larger magnets were employed in a repulsive setup, the pendulum more easily overcame the initial barrier. Furthermore, as the pendulum exited the magnetic field of additional magnets, it experienced a substantial acceleration, which contributed to the increased kinetic energy. This heightened energy level enabled the pendulum to navigate through the subsequent magnetic barriers more effectively.

The results suggest that optimization of the system should involve strategically adjusting the position and strength of repulsive or attractive magnets for a fine tuning of the potential landscape. By doing so, nonlinearities will dominate the dynamics of the pendulum and enhance energy harvesting efficiency. Additionally, a comprehensive understanding of the system's behavior requires investigations on various initial conditions and excitation frequencies. Future works involving such analyses will reveal a spectrum of potential operating regimes, each offering advantages in terms of energy harvesting capabilities. By delving into these aspects, novel strategies for improving the rotational pendulum-based energy harvesting systems can be explored, thereby broadening the practical applications. In our next step, a comprehensive investigation of the model under different angular and axial positions of the side magnets is to be carried out.

Supplementary Materials: The following supporting information can be downloaded at: https://www.mdpi.com/article/10.3390/app14083265/s1, Figure S1: (**a**) Global mesh model of a stationary pendulum and magnet-coil pair. (**b**) Local enlarged mesh view of a stationary pendulum and a magnet-coil pair. (**c**) Contours of magnetic flux density [T] at a distance of −27.5 mm along x-axis; Figure S2: Variation of components of magnet force in x, y, and z axes with the distance between the magnets along x-axis are shown in (**a**–**c**), respectively; Figure S3: Under the application of 1A current through coil, variation of components of magnet force in x, y, and z axes with the distance between the magnets along x-axis are shown in (**a**–**c**), respectively; Figure S4: (**a**) Local mesh of a quasi-dynamic model for a pendulum-magnet and a coil with induced voltage. (**b**) Induced voltage in coil for different speeds of the pendulum. (**c**) Reference characteristics of induced voltage obtained after normalizing with speed; Table S1: List of variables used for the FEA simulation of magnetic force interactions.

Author Contributions: Conceptualization, G.L., M.K., P.W., B.A. and A.M.G.; methodology, G.L., M.K., P.W., B.A. and A.M.G.; software, G.L., M.K. and B.A.; validation, G.L. and M.K.; formal analysis, G.L.; investigation, G.L. and B.A.; resources, B.A.; data curation, G.L., M.K., P.W. and B.A; writing—original draft preparation, G.L., B.A. and A.M.G.; writing—review and editing, G.L., B.A. and A.M.G.; visualization, G.L., M.K., P.W., B.A. and A.M.G.; supervision, G.L.; project administration, P.W. and G.L.; funding acquisition, G.L. All authors have read and agreed to the published version of the manuscript.

Funding: Supported by the National Science Centre, Poland under the project SHENG-2 (Grant No. 2021/40/Q/ST8/00362).

Institutional Review Board Statement: Not applicable.

Informed Consent Statement: Not applicable.

Data Availability Statement: The data presented in this study are available on request from the corresponding author.

Acknowledgments: The authors would like to thank Prof. Shengxi Zhou for useful discussions.

Conflicts of Interest: The authors declare no conflict of interest.

References

1. Kaźmierski, T.J.; Beeby, S. *Energy Harvesting Systems, Principles, Modelling and Applications*; Springer: New York, NY, USA, 2011.
2. Priya, S.; Inman, D.J. *Energy Harvesting Technologies*; Springer: Blacksburg, VA, USA, 2009.
3. Elvin, N.; Erturk, A. *Advances in Energy Harvesting Methods*; Springer: New York, NY, USA, 2013.
4. Yang, T.; Zhou, S.; Litak, G.; Jing, X. Recent advances in correlation and integration between vibration control, energy harvesting and monitoring. *Nonlinear Dyn.* **2023**, *111*, 20525–20562. [CrossRef]
5. Alegret, R.N.; Aragones, R.; Oliver, J.; Ferrer, C. Exploring IIoT and Energy Harvesting Boundaries. In Proceedings of the IECON 2019—45th Annual Conference of the IEEE Industrial Electronics Society, Lisbon, Portugal, 14–17 October 2019; pp. 6732–6736. [CrossRef]
6. Zeadally, S.; Shaikh, F.K.; Talpur, A.; Sheng, Q.Z. Design architectures for energy harvesting in the Internet of Thing. *Renew. Sustain. Energy Rev.* **2020**, *128*, 109901. [CrossRef]
7. Ambrożkiewicz, B.; Litak, G.; Wolszczak, P. Modelling of electromagnetic energy harvester with rotational pendulum using mechanical vibrations to scavenge electrical energy. *Appl. Sci.* **2020**, *10*, 671. [CrossRef]
8. He, J.; Wen, T.; Qian, S.; Zhang, Z.; Tian, Z.; Zhu, J.; Mu, J.; Hou, X.; Geng, W.; Cho, J.; et al. Triboelectric-piezoelectric-electromagnetic hybrid nanogenerator for high-efficient vibration energy harvesting and self-powered wireless monitoring system. *Nano Energy* **2018**, *43*, 326–339. [CrossRef]
9. Zhang, B.; Zhang, Q.; Wang, W.; Han, J.; Tang, X.; Gu, F.; Ball, A.D. Dynamic modelling and structural optimization of a bistable electromagnetic vibration energy harvester. *Energies* **2019**, *12*, 2410. [CrossRef]
10. Cottone, F.; Vocca, H.; Gammaitoni, L. Nonlinear energy harvesting. *Phys. Rev. Lett.* **2009**, *102*, 080601. [CrossRef] [PubMed]
11. Erturk, A.; Inman, D.J. An experimentally validated bimorph cantilever model for piezoelectric energy harvesting from base excitations. *Smart Mater. Struct.* **2009**, *18*, 025009. [CrossRef]
12. Tvedt, L.G.W.; Nguyen, D.S.; Halvorsen, E. Nonlinear behaviour of an electrostatic energy harvester under wide- and narrowband excitation. *J. Microelectromech. Syst.* **2010**, *19*, 305–316. [CrossRef]
13. Zhang, Y.; Wang, T.; Luo, A.; Hu, Y.; Li, X.; Wang, F. Micro electrostatic energy harvester with both broad bandwidth and high normalized power density. *Appl. Energy* **2018**, *212*, 362–371. [CrossRef]
14. Rubes, O.; Brablc, M.; Hadas, Z. Nonlinear vibration energy harvester: Design and oscillating stability analyses. *Mech. Syst. Signal Process.* **2019**, *125*, 170–184. [CrossRef]
15. Aravindan, M.; Ali, S.F. Exploring 1:3 internal resonance for broadband piezoelectric energy harvesting. *Mech. Syst. Signal Process.* **2021**, *153*, 107493. [CrossRef]
16. Haroun, A.; Yamada, I.; Warisawa, S. Study of electromagnetic vibration energy harvesting with free/impact motion for low frequency operation. *J. Sound Vib.* **2015**, *349*, 389–402. [CrossRef]
17. Phan, N.P.; Bader, S.; Oelmann, B. Performance of an electromagnetic energy harvester with linear and nonlinear springs under real vibrations. *Sensors* **2020**, *20*, 5456. [CrossRef] [PubMed]
18. Pepe, G.; Dorla, A.; Roveri, N.; Carcaterra, A. Vibration energy harvesting for cars: Semi-active piezo controllers. *Arch. Appl. Mech.* **2023**, *93*, 663–685. [CrossRef]
19. Cahill, P.; Hazra, B.; Karoumi, R.; Mathewson, A.; Pakrashi, V. Vibration energy harvesting based monitoring of an operational bridge undergoing forced vibration and train passage. *Mech. Syst. Signal Process.* **2018**, *106*, 265–283. [CrossRef]

20. Fan, W.; Zhang, C.; Liu, Y.; Wang, S.; Dong, K.; Li, Y.; Wu, F.; Liang, J.; Wang, C.; Zhang, Y. An ultra-thin piezoelectric nanogenerator with breathable, superhydrophobic, and antibacterial properties for human motion monitoring. *Nano Res.* **2023**, *16*, 11612–11620. [CrossRef]
21. Huang, D.; Zhou, S.; Han, Q.; Litak, G. Response analysis of the nonlinear vibration energy harvester with an uncertain parameter. *Proc. Inst. Mech. Eng. Part K J. Multi-Body Dyn.* **2020**, *234*, 393–407. [CrossRef]
22. Malaji, P.V.; Ali, S.F. Broadband energy harvesting with mechanically coupled harvesters. *Sens. Actuators A* **2017**, *255*, 1–9. [CrossRef]
23. Kullah, H.; Najafi, K. Energy Scavenging from Low-Frequency Vibrations by Using Frequency Up-Conversion for Wireless Sensor Applications. *IEEE Sens. J.* **2008**, *8*, 261–268. [CrossRef]
24. Jia, Y. Review of nonlinear vibration energy harvesting: Duffing, bistability, parametric, stochastic and others. *J. Intell. Mater. Syst. Struct.* **2020**, *31*, 921–944. [CrossRef]
25. Giri, A.M.; Ali, S.F.; Arockiarajan, A. Characterizing harmonic and subharmonic solutions of the bi-stable piezoelectric harvester with a modified harmonic balance approach. *Mech. Syst. Signal Process.* **2023**, *198*, 110437. [CrossRef]
26. Ferrari, M.; Ferrari, V.; Guizzetti, M.; Ando, B.; Baglio, S.; Trigona, C. Improved energy harvesting from wideband vibrations by nonlinear piezoelectric converters. *Sens. Actuators A Phys.* **2010**, *162*, 425–431. [CrossRef]
27. Huguet, T.; Badel, A.; Lallart, M. Exploiting bistable oscillator subharmonics for magnified broadband vibration energy harvesting. *Appl. Phys. Lett.* **2017**, *111*, 173905. [CrossRef]
28. Pellegrini, S.P.; Tolou, N.; Schenk, M.; Herder, J.L. Bistable vibration energy harvesters: A review. *J. Intell. Mater. Syst. Struct.* **2013**, *24*, 1303–1312. [CrossRef]
29. Giri, A.M.; Ali, S.F.; Arockiarajan, A. Influence of asymmetric potential on multiple solutions of the bi-stable piezoelectric harvester. *Eur. Phys. J. Spec. Top.* **2022**, *231*, 1443–1464. [CrossRef]
30. Dong, L.; Closson, A.B.; Jin, C.; Trase, I.; Chen, Z.; Zhang, J.X.J. Vibration-Energy-Harvesting System: Transduction Mechanics, Frequency Tuning Techniques and Biomechanical Applications. *Adv. Mater. Technol.* **2019**, *4*, 1900177. [CrossRef] [PubMed]
31. Bouhedma, S.; Rao, Y.; Schutz, A.; Yuan, C.; Hu, S.; Lange, F.; Bechtold, T.; Hohfeld, D. System-Level Model and Simulation of a Frequency-Tunable Vibration Energy Harvester. *Micromachines* **2020**, *11*, 91. [CrossRef] [PubMed]
32. Huguet, T.; Lallart, M.; Badel, A. Orbit jump in bistable energy harvesters through buckling level modification. *Mech. Syst. Signal Process.* **2019**, *128*, 202–215. [CrossRef]
33. Lee, S.; Lee, Y.; Dongseob, K.; Yan, Y.; Lin, L.; Lin, Z.H.; Hwang, W.; Wang, Z.L. Triboelectric nanogenerator for harvesting pendulum oscillation energy. *Nano Energy* **2013**, *2*, 1113–1120. [CrossRef]
34. Xu, J.; Tang, J. Multi-directional energy harvesting by piezoelectric cantilever-pendulum with internal resonance. *Appl. Phys. Lett.* **2015**, *107*, 213902. [CrossRef]
35. Wu, Y.; Qiu, J.; Shengpeng, Z.; Ji, H.; Chen, Y.; Li, S. A piezoelectric spring pendulum oscillator used for multi-directional and ultra-low frequency vibration energy harvesting. *Appl. Energy* **2018**, *231*, 600–614. [CrossRef]
36. Wang, Y.J.; Chen, C.D.; Sung, C.K. Design of a frequency-adjusting device for harvesting energy from a rotating wheel. *Sens. Actuators A* **2010**, *159*, 196–203. [CrossRef]
37. Naifar, S.; Bradai, S.; Viehweger, C.; Kanoun, O. Survey of electromagnetic and magnetoelectric vibration energy harvesters for low frequency excitation. *Measurement* **2017**, *106*, 251–263. [CrossRef]
38. Yurchenko, D.; Alevras, P. Parametric pendulum based wave energy converter. *Mech. Syst. Signal Process.* **2018**, *99*, 504–515. [CrossRef]
39. Malaji, P.V.; Ali, S.F. Analysis of energy harvesting from multiple pendulums with and without mechanical coupling. *Eur. Phys. J. Spec. Top.* **2015**, *224*, 2823–2838. [CrossRef]
40. Malaji, P.V.; Doddi, S.; Friswell, M.I.; Adhikari, S. Analysis of pendulums coupled by torsional springs for energy harvesting. *MATEC Web Conf.* **2018**, *211*, 05008. [CrossRef]
41. Kuang, Y.; Hide, R.; Zhu, M. Broadband energy harvesting by nonlinear magnetic rolling pendulum with sub-harmonic resonance. *Appl. Energy* **2019**, *255*, 113822. [CrossRef]
42. Dai, X. An vibration energy harvester with broadband and frequency-doubling characteristics based on rotary pendulums. *Sens. Actuators A Phys.* **2016**, *241*, 161–168. [CrossRef]
43. Koszewnik, A. Analytical Modeling and Experimental validation of an energy harvesting system for the smart plate with and integrated piezo-harvester. *Sensors* **2019**, *19*, 812. [CrossRef]
44. Borowiec, M.; Syta, A.; Litak, G. Energy harvesting optimizing with a magnetostrictive cantilever beam system. *Int. J. Struct. Stab. Dyn.* **2019**, *19*, 1941002. [CrossRef]
45. Smilek, J.; Hadas, Z.; Vetiska, J.; Beeby, S. Rolling mass energy harvester for very low frequency of input vibrations. *Mech. Syst. Signal Process.* **2019**, *125*, 215–228. [CrossRef]
46. Toyabur, R.M.; Salauddin, M.; Cho, H.; Park, J.Y. A multimodal hybrid energy harvester based on piezoelectric-electromagnetic mechanisms for low-frequency ambient vibrations. *Energy Convers. Manag.* **2018**, *168*, 454–466. [CrossRef]
47. Li, Z.; Yan, Z.; Luo, J.; Yang, Z. Performance comparison of electromagnetic energy harvesters based on magnet arrays of alternating polarity and configuration. *Energy Convers. Manag.* **2019**, *179*, 132–140. [CrossRef]

48. Cui, X.; Hu, J. An infrasonic vibration energy harvester using pendulum impact. *Int. J. Appl. Electromagn. Mech.* **2015**, *47*, 467–474. [CrossRef]
49. Avila Bernal, A.G.; Linares Garcia, L.E. The modelling of an electromagnetic energy harvester architecture. *Appl. Math. Model.* **2012**, *36*, 4728–4741. [CrossRef]